The Egyptian Journal of Hospital Medicine (January 2023) Vol. 90, Page 1087-1097

Diagnostic and Interventional Role of Magnetic Resonance Imaging and Ultrasound in Painful Wrist Conditions

Nouran Abd Al Aziz Al Aswad*[1], Samah Ahmed Radwan[1], Mohamed Ahmed Esmail[1], Hanan Mohamed El-Saadany[2], Atef Hammad Teama[1]

Departments of [1]Radiodiagnosis and [2]Physical Medicine, Rheumatology and Rehabilitation, Faculty of Medicine, Tanta University, Tanta, Egypt

***Corresponding author:** Nouran Abd Al Aziz Al Aswad, **Mobile:** (+20) 01120914330,

E-Mail: nouran.alaswad@med.tanta.edu.eg

ABSTRACT

Background: Ultrasound (US) is the best technique for imaging tendons as it allows dynamic tendon examination. Magnetic Resonance Imaging (MRI) can be utilized to enhance detection and evaluation of several wrist disorders. Magnetic Resonance arthrography (MRA) is the modality of choice for triangular fibrocartilage complex (TFCC) assessment. **Objective:** The aim of this work was to evaluate diagnostic and interventional management of MRI and US in painful wrist conditions.

Patients and Methods: This prospective study was carried out on 50 patients aging from 12 to 66 years with wrist pain. All patients were subjected to MRI, MRA and US examination.

Results: US predicted bone fracture, ganglion cysts, late avascular necrosis, first, second, third, fourth and sixth (extensor carpi ulnaris) compartment tendon involvement, flexor tendon injury, median nerve involvement, rheumatoid arthritis and osteoarthritic changes.

Conclusions: US showed promising results regarding the examination of superficial bony and soft tissue structures of the wrist. However, MRI is better for evaluation of internal wrist derangement. Ultrasound is also highly operator dependent. MRA is highly accurate for the evaluation of TFCC and ligamentous injury of the wrist joint.

Keywords: Magnetic Resonance Imaging, Ultrasound, Wrist Conditions.

INTRODUCTION

Pain in the wrist can be either acute, occurring suddenly after an accident, or subacute, occurring gradually over time, with or without an acute injury [1]. The evaluation of patients with wrist and hand discomfort might reveal a wide range of pathologic disorders. Tenosynovitis, trigger finger, De Quervain's disease, and ganglion cyst are a few examples of these disorders[2].

The most accurate method of visualizing tendons is ultrasound (US). Its ability to examine tendons in motion is a significant improvement over MRI [1]. US is preferable to MRI and CT for evaluating peripheral nerves because it provides more clear pictures [3].

Tendon sheaths, which are used for injecting drugs into joints, are useful in the treatment of many different conditions. Recent advances have made US a viable imaging modality due to its low cost, high efficiency, and lack of radiation [4]. So, as to direct less invasive percutaneous methods for the treatment of certain diseases [5,6].

The primary goals of US-guided interventional therapies are symptom management and postponement or elimination of surgical intervention [7].

Since MRI can distinguish between bone marrow, ligaments, tendons, cartilage, muscles, nerves, and blood vessels, it can be used to improve the detection and evaluation of numerous wrist disorders [8]. The triangular fibrocartilage should be evaluated with a magnetic resonance arthrogram (MRA) after gadolinium-containing contrast material has been injected (TFC). TFC evaluations are best performed by MRA [9].

This research aimed to compare the effectiveness of MRI and US for diagnosing and treating painful wrist problems that required intervention.

PATIENTS AND METHODS

In this prospective study, we looked at 50 patients, with ages ranging from 12 to 66 years old (34 males and 16 females). During the 24 months from January 2020 to May 2022, patients from the Orthopedics and Physical Medicine and Rehabilitation Departments at the Faculty of Medicine at Tanta University Hospital were referred to the Radiodiagnosis Department for ultrasonography and MRI examinations (with the exception of 5 cases, who were examined in the Radiodiagnosis Department at Cairo University Hospital).

This research enrolled participants who were experiencing wrist pain.

Patients intolerant of contrast administration, particularly those with compromised renal functions, patients who are claustrophobic, and patients who cannot have an MRI test due to a pacemaker, a critically positioned metallic foreign body, or incompatible vascular implants were excluded.

Orthopedic and Physical Medicine Departments at Tanta University Hospitals and, in 5 cases, at Cairo University Hospitals conducted thorough examinations and reviewed all available investigations for all patients. MR arthrography was conducted in 9 cases, and US guided operations were performed in 13 cases, all with high resolution US examination, MRI (1.5 T) examination with or without IV contrast according to the indications. When possible, we also compared our

Received: 01/08/2022
Accepted: 02/10/2022

findings to those from surgeries, arthroscopies, and autopsies.

Ultrasonographic examination:

In both the Physical Medicine and Radiology Departments at Cairo University Hospitals, high-frequency linear probes of Samsung MEDISON UGEOH60 (5-13 MHz) were used for US tests; in 5 cases, GE Logic pro6 (7-11 MHz) was used instead.

Dorsal approach:

Once we've located the Lister's tubercle at the distal radius, a bony landmark that divides the lateral and medial compartments, the probe was moved laterally on transverse planes to see the extensor tendons of the lateral compartment in axial view, and then the probe was rotated about 90 degrees to see the tendons in long axis view. In order to access the third compartment on the medial side of the Lister tubercle, the probe was moved laterally. The first compartment was checked by placing the probe on the lateral surface of the radial styloid with the patient's wrist in a position midway between pronation and supination. The transducer was positioned on a transverse plane above the middle of the dorsal wrist in order to check out the fourth compartment and the medial portion of the fifth compartment. Slight radial displacement of the wrist was used to access the sixth compartment. We examined the ulnar styloid process as well as the triangular fibrocartilage complex that bridges the gap between the ulna and the radius (TFCC). The transducer was positioned longitudinally on the ulnar side of the wrist, above the notch between the distal ulna and triquetrum; next, the transducer was slid to provide a coronal picture of the TFCC; radial deviation was essential for recognizing the cartilage. Transverse planes were used to transfer the probe distally from the level of the Lister tubercle in order to view the dorsal section of the scapholunate ligament. If the examiner wants to get a good look at this ligament, deviating his wrist to the ulnar side was tried. Between the scaphoid and lunate, it manifests as a triangle echogenic structure. To find the lunotriquitral, the probe was moved ulnarly down the transverse axis until it is. The distal radioulnar joint was inspected by angling the probe in the transverse plane so that it was closer to the joint's proximal end than the joint's distal end. For this reason, we focused on the hyperechogenecity of the carpal bones to analyze the radiocarpal and midcarpal joints.

Volar approach:

Patients were instructed to maintain their dorsal wrist facing the examiner so that the proximal carpal tunnel could be inspected. To locate the proximal carpal tunnel's bony markers, we positioned the probe across the palmar crease in the axial plane and felt for the scaphoid tubercle (radial side) and pisiform (ulnar side). The flexor retinaculum and the median nerve (found beneath it, superficial to the flexor tendons of the second and third fingers, and medial to the flexor pollicis longus) were examined. Cross-sectional measurements of the proximal and distal carpal tunnels were used to determine the median nerve's circumference. Typically, the proximal carpal tunnel was used to measure the median nerve's mean cross-sectional area, and this number shouldn't exceed 12 mm.

The transverse plane at the distal carpal tunnel level provides the highest flattening ratio for the nerve. The ideal ratio is one that is lower than 3. The carpal tunnel houses nine long flexor tendons. The flexor carpi radialis tendon, which sits above the hyperechoic cortex of the scaphoid and is therefore at the radial side of the carpal tunnel, was examined.

Moving the probe to a more distal transverse plane allowed us to locate the trapezium tubercle (radial side) and hamate hook, two bone features of the distal carpal tunnel (ulnar sided). We turn the transducer such that its tip points medially on the transverse plane so that we can see the Guyon's canal and the ulnar nerve.

MRI:

Tanta University Hospital's Radiology Department used a Toshiba vintage Titane (1.5 T) and a GE 1.5 Tesla (SIGNA explorer) to perform MRI on 45 patients, whereas the Radiology Department at Kasr El-Eini Hospital, Cairo University, used a Philips Achieva or Intera (1.5 T) for 5 patients. Patients were asked to take out any jewelry that contained metal, such as stud earrings or pins. Putting the patient at ease by thoroughly explaining the examination's steps, position, and duration, with an emphasis on maintaining complete stillness throughout. In all five scans performed at the Radiology Department of Cairo University's Kasr El-Eini Hospital, the patients were scanned while lying on their stomachs with their arms raised above their heads using a flex coil and a dedicated wrist coil.

Prior to the axial shimming (13 seconds) and FE map (31 seconds), preliminary scout localizers were obtained in the axial, coronal, and sagittal planes for approximately 33, 26 and 26 seconds, respectively. Localizer images are crucial for planning various sequences.

Sequences of magnetic resonance imaging (Tanta University Hospital): Axial (T1, T2 WIs, and PDFAT SAT), coronal (T1, T2 WIs, PD FAT SAT, T2*, and STIR), sagittal (T2 WI 3D), SAGITTAL (PD FAT SAT), T1 FAT SAT, and STIR post-contrast) pulse sequences were used in the MRI investigation

contrast (axial, Sagittal and coronal planes) (axial, Sagittal and coronal planes). The subsequent constraints were used: Matrix size 224 x 256 pixels and field of view 14 x 14 cm, number of slices 20, no wrap, flip angle 90; slice thickness 3 mm; interslice gap 0.3 mm. Twenty-five minutes was the average length of the test **(Table 1)**.

Table (1): MRI sequences parameters (Tanta University Hospital)

Sequence	TR (msec)	TE (msec)	Flip Angle (º)
PDFAT SAT	3400	12	90
T1 FSE +10	680	10	90
T2	3400	84	90
GRE T1	Variable	< 30	70-110
GRE T2*	680	9	25
FSE STIR	4365	72	180 -> 90
SAGITTAL T2 STIR	7525	80	90~160
SAGITTAL T2FATSAT	3300	60	90

Sagittal PD SPAIR Wis, Axial T1 and T2WIs, coronal T1, PD SPAIR and 3D WATSWIs, T1 SPAIR post contrast (axial, Sagittal, and coronal planes) if employed, were all part of the MRI study performed at Cairo University Hospital **(Table 2)**.

Table (2): MRI sequences parameters (Cairo University Hospital)

Parameters	Axial T1	Axial T2	Sagittal PD SPAIR	Coronal T1	Coronal PD SPAIR	Coronal 3D WATS
TE	**22**	**100**	**30**	**22**	**30**	**8**
TR	**533**	**4600**	**6100**	**450**	**3900**	**20**

Field of view varied from 80 to 100 mm, and slices were 2.5 mm thick with a 0.3 mm gap (except for the coronal 3D WATS sequence, in which the slices were 1.5 mm thick with a -0.8 mm gap).

MRA [10]:

In 9 cases, MRA was performed because it was medically necessary. We used this method to get the job done. In the Radiology Department of Kasr El-Eini Hospital, Cairo University, and the GE C-Arm at Tanta University Hospital, MRA procedures were performed under fluoroscopy guidance. Patients were positioned supine with their forearms pronated, and the contrast mixture was injected using a dorsal technique. Betadine solution was used to disinfect the area before it was draped off. An injection of a 0.5% solution of xylocaine was used to produce temporary numbness in the subcutaneous tissue. We combined 0.1 ml of gadopentetate dimeglumine with 3 ml of non ionic contrast medium, 5 ml of xylocaine, and 10 ml of sterile saline solution to make a 20 ml combination.

A 22-gauge needle on a 5-centimeter syringe was inserted dorsally into the scaphocapitate space of the midcarpal joint, and the injection was continued until the contrast was seen in the capitolunate joint area. When leakage into the radiocarpal joint was observed, just a single injection into the mid carpal joint was performed; otherwise, both the mid carpal and radiocarpal joints were injected.

The radiocarpal joint was flexed over a sponge, and the needle was inserted perpendicular to the joint, 0.5 cm distal to Lister's tubercle on the dorsum of the radius. After injecting 3–4 ml of contrast mixture into the mid carpal compartment, the patient should feel pressure within the joint. If communication with the DRUJ has been established, an additional 4-5 ml may be injected into the carpal region. After 30 minutes, the patients were brought to the MRI unit, during which time they were instructed to actively exercise the joint to spread the contrast about.

T1 fat suppression sequences were performed in the coronal, axial, and sagittal planes, all using the same specialized wrist coil. The structures of the hand and wrist were meticulously examined.

US guided injections:

Radiocarpal joint injection in case of osteoarthritis was done using inplane approach, the needle was inserted into the joint space directed toward the radius with injection of 2 ml mixture of corticosteroid and lidocaine.

US-Guided first extensor compartment tendon sheath injection in case of dequervain's disease was done by placing the probe transversely over the radial styloid process, the needle was inserted from the ulnar side to avoid radial artery injury, then passing deep to the tendons and 1 ml mixture of corticosteroid and lidocaine was injected into the tendon sheath.

When treating ECU tenosynovitis with an out-of-plane method, the probe was positioned longitudinally on the ulnar side of the wrist, and the needle was inserted under the tendon sheath of ECU; then, 1 ml of mixture was injected beneath the tendon sheath.

US-Guided TFCC injection was done using in plane approach, simply by putting the probe in the right spot horizontally over the dorsal wrist, the needle was advanced deep to ECU tendon to reach the TFCC, compounded from a variety of corticosteroid and a shot of lidocaine was administered to the degenerated TFCC.

US-Guided carpal tunnel injection was done by inserting the needle through the flexor retinaculum and injection of 2 ml mixture above and below the median nerve.

US-Guided Aspiration of ganglion cysts was done using wide pore cannula and 10 cm syringe, in one case aspiration failed to empty the cyst because the content was highly viscous so the other option was piercing the

cyst walls by needle in different directions, which leads to cyst self-decompression.

Ethical approval:

The Ethical Committee of Tanta University Hospitals gave their support to the project. Adult patients' written informed consent was acquired, while the parents of children patients gave their written consent. This study was conducted in compliance with the Code of Ethics of the World Medical Association (Declaration of Helsinki) for human subjects.

Statistical analysis

The data were statistically described using case counts and percentage breakdowns. Kappa analysis was used to evaluate the correlation between ultrasound (US) and magnetic resonance imaging (MRI). With regards to statistics, a p-value of 0.05 or less was considered to be significant. All statistical analyses were performed using SPSS (Statistical Package for the Social Sciences; SPSS Inc., Chicago, IL, USA) version 15 for Microsoft Windows (2006).

RESULTS

There was a highly significant agreement (p value <0.001) between both modalities in the detection of bony fractures, ganglion cyst and avascular necrosis **(Table 3)**.

Table (3): Comparison between MRI and US in the detection of bony fractures, ganglion cysts, late avascular necrosis

Bone fracture by ultra-sonography	**Bone fracture by MRI**		**P value**
	Positive	**Negative**	
Positive	18 (100 %)	0 (0 %)	**<0.001***
Negative	0 (0 %)	32 (100 %)	
Ganglion cyst by ultra-sonography	**Ganglion cyst by MRI**		**P value**
	Positive	**Negative**	
Positive	16 (100 %)	0 (0 %)	**<0.001***
Negative	0 (0 %)	34 (100 %)	
Avascular necrosis by ultra- sonography	**Avascular necrosis by MRI**		**P value**
	Positive	Negative	
Positive	11 (100 %)	0 (0 %)	**<0.001***
Negative	0 (0 %)	39 (100 %)	

Data are presented as frequency (%), * significant, MRI: Magnetic resonance imaging, US: Ultrasound

The MRI detected TFCC injury in 16 joints while ultrasound detected lesions in 14 joints, they both agreed in 48 joints, ultrasound missed TFCC injury in two joints. Statistical analysis of the results showed highly significant agreement (p value <0.01) between the two modalities in the detection of triangular fibrocartilage (TFCC) tear. Nine patients underwent MRA, MRA detected TFCC injury in 6 joints while MRI detected it in 4 joints. MRI missed 2 joints that were detected by MRA. Both agreed in 7 joints. Statistical analysis of the results showed P value = 0.058 which was not significant due to small sample size (**Table 4)**.

Table (4): Comparison between MRI and ultrasound in the detection of TFCC injury and degeneration (33) and comparison between MRI and MRA in the detection of TFCC tear and degeneration

TFCC lesions detected by US	**TFCC lesions detected by MRI**				**Total**	
	Positive		**Negative**			
	n	%	n	%	n	%
Positive	34	100.0	2	12.5	36	72.0
Negative	0	0.0	14	87.5	14	28.0
Total	34	100.0	16	100.0	50	100.0
Sensitivity = 100.0%	Specificity = 87.5%		PPV = 94.4%		NPV= 110.0%	
TFCC lesions detected by MRA	**TFCC lesions detected by MRI**				**Total**	
	Positive		**Negative**			
	n	%	n	%	n	%
Positive	3	60.0	0	0.0	3	33.3
Negative	2	40.0	4	100.0	6	66.7
Total	5	100.0	4	100.0	9	100.0
Sensitivity = 60.0%	Specificity = 100.0%		PPV = 100.0%		NPV= 66.7%	

MRA detected ligament tear in 5 joints while MRI detected it in 3 joints. They both agreed in 48 joints. MRI missed 2 joints with ligament tear detected by MRA. The MRI detected ligament injury in 8 joints while ultrasound detected it in the same joints Statistical analysis of these results showed highly significant statistical agreement (p value <0.01) between the two modalities in the detection of ligament injury (**Table 5)**.

Table (5): Comparison between MRI and MRA for the detection of ligament tear and validity of detection of ligamentous tear by ultrasonography as compared to MRI as golden standard

MRA ligament	Ligamentous tear by MRI				Total	
	Positive		Negative			
	n	%	n	%	n	%
Positive	1	25.0	0	0.0	1	11.1
Negative	3	75.0	5	100.0	8	88.9
Total	4	100.0	5	100.0	9	100.0
Sensitivity = 25.0%	Specificity = 100.0%		PPV = 100.0%		NPV= 62.5%	
Ligamentous tear by ultra-sonography						
	n	%	n	%	n	%
Positive	8	100.0	0	0.0	8	16.0
Negative	0	0.0	42	100.0	42	84.0
Total	8	100.0	42	100.0	50	100.0
Sensitivity = 100%	Specificity = 100.0%		PPV = 100.0%		NPV= 100%	Kappa =1.000, p<0.001

There was a highly significant agreement (p value <0.001) between both the MRI and US for the detection of first, second, third, fourth and sixth compartment extensor tendon and ECU injury as well as flexor tendon involvement (**Table 6)**.

Table (6): Comparison between MRI and US in the detection of first, second, third, fourth, Sixth (ECU) compartment and flexor tendon involvement (tenosynovitis)

First extensor tendon involvement by ultra-sonography	First extensor tendon involvement by MRI		P value
	Positive	Negative	
Positive	3 (100 %)	0 (0 %)	<0.001*
Negative	0 (0 %)	47 (100 %)	
Second extensor tendon involvement by ultra-sonography	**Second extensor tendon involvement by MRI**		**P value**
	Positive	**Negative**	
Positive	9 (100 %)	0 (0 %)	<0.001*
Negative	0 (0 %)	41 (100 %)	
Third extensor tendon involvement by ultra-sonography	**Third extensor tendon involvement by MRI**		**P value**
	Positive	**Negative**	
Positive	2 (100 %)	0 (0 %)	<0.001*
Negative	0 (0 %)	48 (100 %)	
Fourth extensor tendon involvement by ultra-sonography	**Fourth extensor tendon involvement by MRI**		**P value**
	Positive	**Negative**	
Positive	2 (100 %)	0 (0 %)	<0.001*
Negative	0 (0 %)	48 (100 %)	
Sixth extensor tendon (ECU) involvement by ultra-sonography	**Sixth extensor tendon (ECU) involvement by**		**P value**
	Positive	**Negative**	
Positive	7 (100 %)	0 (0 %)	<0.001*
Negative	0 (0 %)	43 (100 %)	
Flexor tendon involvement by ultra-sonography	**Flexor tendon involvement by MRI**		**P value**
	Positive	**Negative**	
Positive	4 (100 %)	0 (0 %)	<0.001*
Negative	0 (0 %)	46 (100 %)	

Data are presented as frequency (%), * significant. MRI: Magnetic resonance imaging, US: Ultrasound, ECU: Extensor carpi ulnaris

Both MRI and US agreed in detection of carpal tunnel syndrome. There was a highly significant agreement (p value <0.001) between both MRI and US **(Table 7)**.

Table (7): Comparison between MRI and US in the detection of median nerve involvement (carpal tunnel syndrome) proven by EMG

Median nerve involvement by ultra-sonography	Median nerve involvement by MRI		P value
	Positive	Negative	
Positive	7 (100 %)	0 (0 %)	<0.001*
Negative	0 (0 %)	43 (100 %)	

Data are presented as frequency (%), * significant, MRI: Magnetic resonance imaging, US: Ultrasound

Four cases out of 50 showed advanced rheumatoid arthritis, both US and MRI agreed in detection of all signs of advanced rheumatoid arthritis. Comparison between MRI and US in the detection of osteoarthritic changes revealed a highly significant agreement (p value <0.001) (**Table 8)**.

Table (8): Comparison between MRI and US for the detection of signs of late rheumatoid arthritis and osteoarthritic changes

Rheumatoid arthritis by ultra-sonography	Rheumatoid arthritis by MRI		P value
	Positive	Negative	
Positive	4 (100 %)	0 (0 %)	<0.001*
Negative	0 (0 %)	46 (100 %)	
Osteoarthritis by ultra-sonography	**Osteoarthritis by MRI**		**P value**
	Positive	Negative	
Positive	14 (100 %)	0 (0 %)	<0.001*
Negative	0 (0 %)	36 (100 %)	

Data are presented as frequency (%), * significant, MRI: Magnetic resonance imaging, US: Ultrasound

Figures 1-3 show the findings in 3 different patients.

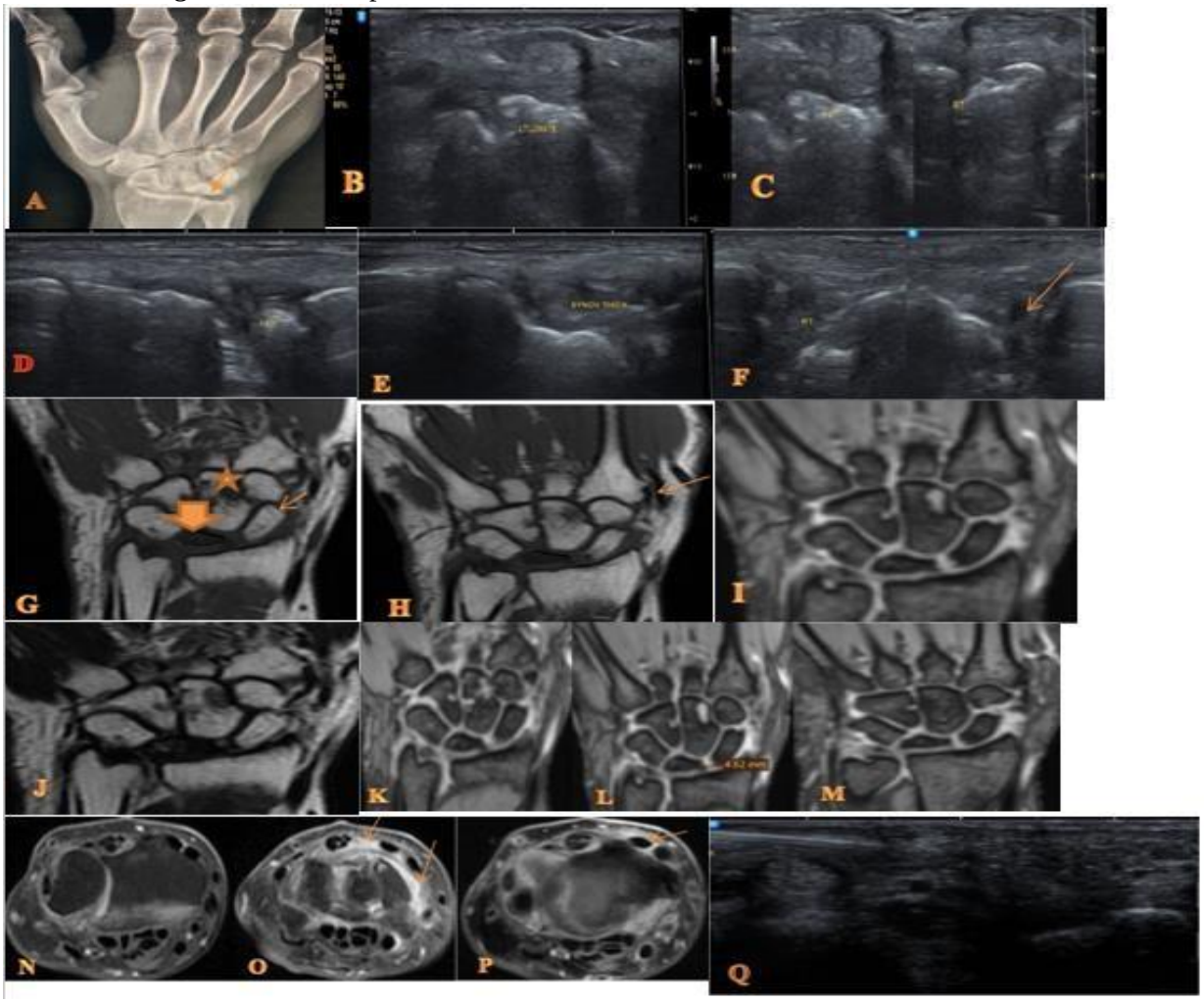

Figure (1): A) X-ray of the wrist (AP view) revealed sclerosis and decreased height of lunate (marked by thin arrow), B), C), D) ultrasound images of the left lunate bone showing increased echogenicity and bony irregularity, E), F) longtudinal ultrasound images showing synovial thickening , ill defined hypoechoic area in left TFCC marked by thin arrow suggesting its degeneration, G), H) coronal T1WI images : marked structural collapse of lunate with hypointense signal (marked by thick arrow) in addition to carpal erosions, osteophytes in the triquetrum and head of second metacarpal bone, I), J) coronal T2 * WI and T2 WI MRI images : hypointense signal of lunate bone in T2WI. Mild wrist effusion, K), L), M) coronal T2 * WI images: Slightly widened scapholubnate interval suggesting scapholunate ligament partial tear. Wearing and abnormal high signal of triangular fibrocartilage associated with minimal fluid in the distal radioulnar joint, N), O), P) Axial PD FAT SAT images showed diffuse synovial thickening and fluid signal around 2nd and 4th extensor compartment tendons (marked by arrows), Q) ultrasound guided injection. Diagnosis: Kienbock's disease - scapholunate ligament partial injury - Degenerative TFCC injury class II c - Secondary wrist osteoarthritic changes - Mild 2nd and 4th extensor compartment tenosynovitis.

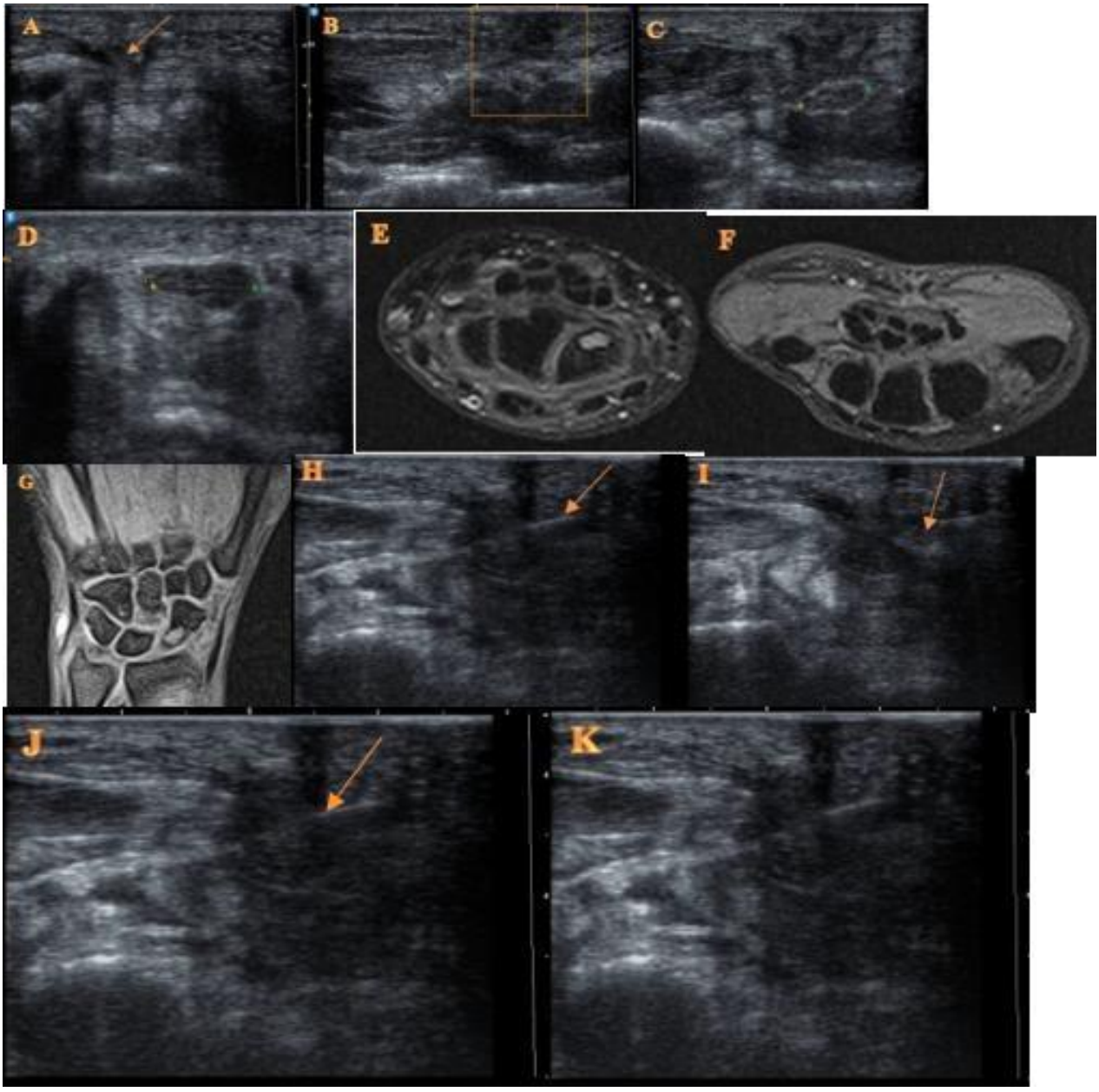

Figure (2): A), B) longitudinal ultrasound images of the carpal tunnel showing hyperechoic granulation tissue compressing the median nerve at the site of incision (marked by arrow) with no colour flow on color Doppler study, C), D) transverse ultrasound images of carpal tunnel showing swelling of the median nerve with increased surface area reaching 0.3 cm^2 at its maximum dimensions, E), F) axial PD FAT SAT MRI images of the wrist showing swelling of the median nerve at the proximal carpal tunnel with flattening and compression of the median nerve at the site of operative incision by hyperintense granulation tissue, G) Coronal PD FAT SAT MRI image of the wrist showing scaphoid cyst and subtle wrist effusion, H), I), J), K) serial images of ultrasound guided injection at the site of compressing grannulation tissue by corticosteroids (marked by thin arrows). Diagnosis: Recurrent carpal tunnel syndrome (granulation and fibrous tissue compressing the median nerve).

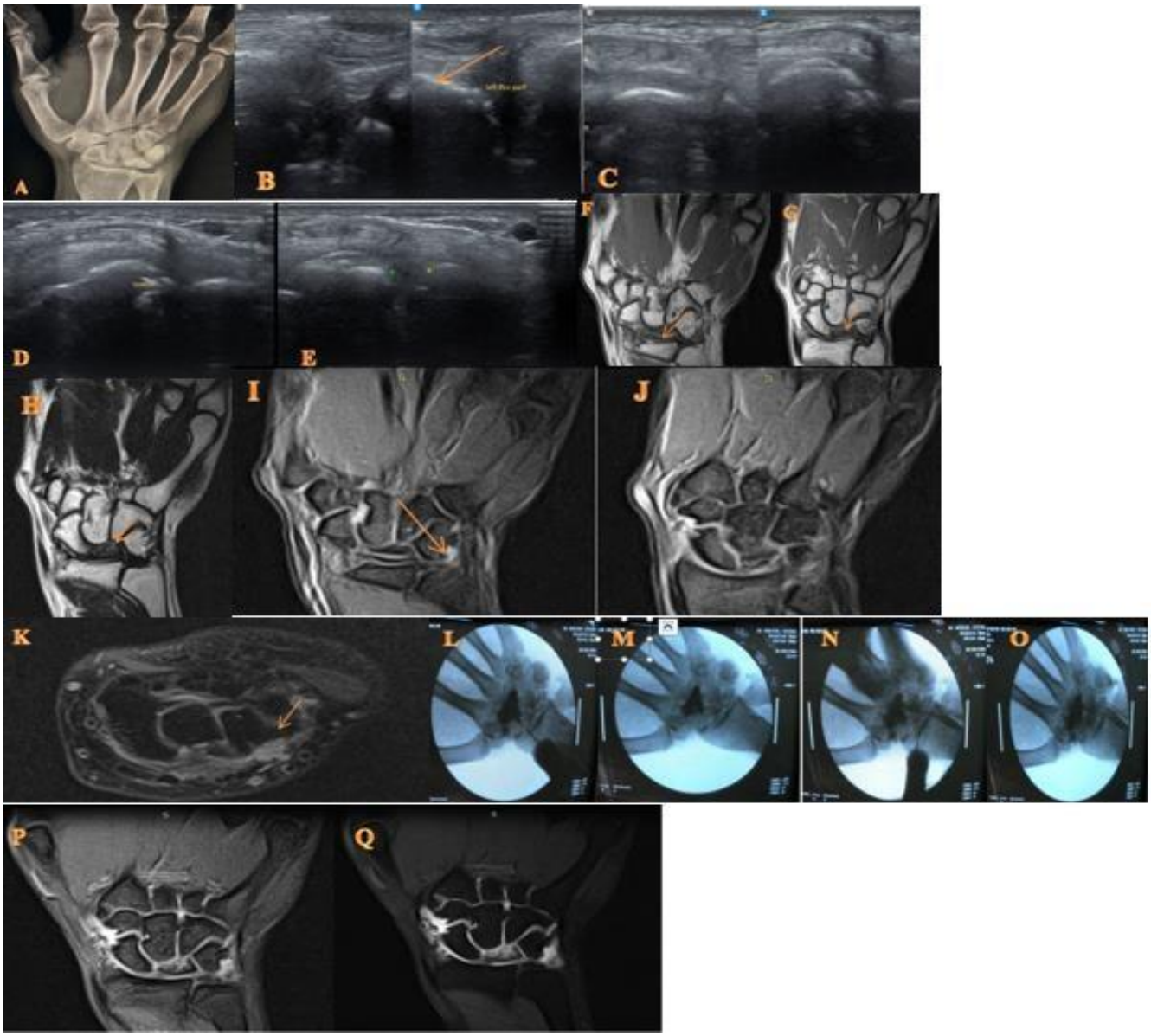

Figure (3): A) plain X-ray of the wrist (AP) showing decreased height and sclerosis of the lunate, B) coronal ultrasound image showing decreased echogenicity of left TFCC incomparison to the right one with hypoechoic area and discontinuity in the articular disc with hypoechoic area representing TFCC tear (thin arrow). C), D) irregularity and increased echogenicity of lunate bone in comparison to the other side E) slightly widened scapholunate distance measuring about 4.6 mm, F), G), H) coronal T1WI and T2WI MR images showing structural collapse of the lunate in the form of decreased height implicating over linear fracture lines with decreased its signal intensity in both T1WI and T2WI (thin arrows), slightly widened scapholunate distance and mild negative ulnar variance, I) J) coronal T2* MR images showing two linear fracture lines involving lunate bone with suspected central tear in the TFCC (thin arrow) and mild wrist effusion, K) Axial PDFAT SAT MR image showing dorsal extraarticular ganglion cyst (thin arrow), L), M), N), O) serial radiographic images of intraarticular contrast injection L, M: midcarpal injection N, O: radiocarpal injection, P), Q) Coronal T2* and T1WI with FATSAT post arthrography showing central tear at articular disc of triangular fibrocartilage. Diagnosis: kienbock's disease, central tear of triangular fibrocartilage (Palmer class I a), dorsal ganglion cyst.

DISCUSSION

In the present study, all patients were suffering from wrist pain. 15 cases (30%) suffered from acute pain while 35 cases (70%) suffered from chronic pain and 31 cases (62 %) had swelling. 32 cases (64%) had a history of trauma. It was found that our findings agreed with those of **El-Deek *et al.*** [11] who found that 32 patients (or 64%) out of 50 reported having experienced trauma in the past.

In the present study, according to clinical diagnosis, the most common lesion was found in 18 cases (36%) who had TFCC lesions and fractures followed by 16 (32%) with ganglion cysts and 9 (18%) with 2nd compartment tenosynovitis. In **El-Deek *et al.*** [11] study, There were a total of 50 patients, and their diagnoses ranged from tendinopathy (40%), to TFCC tears (16%), to simple ganglions (16%), to solid masses (6%), to foreign bodies (4%), to CTS (18%). However, **Singh *et al.*** [12] observed ganglion cysts were the most prevalent pathological finding, occurring in 29 patients (36 percent). This discrepancy between our findings and theirs may be attributable to differences in lifestyle since their research was done in India plus occupational factors.

TFCC injury or degeneration was discovered by MRI in 16 joints but only by US in 14 joints, hence there was a high degree of agreement between the two methods in the present investigation. Our results are supported by **Kadry *et al.*** [13] who reported that wrist discomfort or reduced wrist mobility was reported by 35 individuals with a mean age of 39 ± 13.18 years old. The US detected 18 positive cases with TFCC injury with a percentage of 51.4%. The MRI detected 24 positive cases with TFCC injury with a percentage of 68.6%. The ultrasound had a 75% sensitivity, 100% specificity, 100% PPV, and a 64.7 NPV for detecting TFCC patients.

While we found no evidence of TFCC tears on ultrasonography (USG), **El-Deek *et al.*** [11] found that MRI properly detects its diseases (75% sensitivity). This discrepancy may be due to the fact that MRI, the gold standard, permits assessment of soft tissue involvement, which may account for the findings of the two investigations.

In the current investigation, TFCC damage was found in 6 joints using MRA and 4 joints using MRI. While MRA was able to identify two joints affected by TFCC damage, MRI had missed them both. With regards to evaluating TFCCs, MRA was the method of choice. Our results are consistent with those of **Kadah *et al.*** [14] who examined the diagnostic accuracy of magnetic resonance arthrography and magnetic resonance imaging for TFCC and other intrinsic ligaments of the wrist tear evaluation. 57 patients who complained of wrist pain underwent MRI and MRA were included. The diagnostic accuracy of arthroscopy was shown to be superior. The results of their research demonstrated the superiority of MR arthrography over MRI in the diagnosis of ligamentous diseases.

Our results are incompatible with **El-Deek *et al.*** [11] who reported that USG was able to identify simple ganglion in 6 of 8 (75%) and solid mass lesions in all 3 (100%) of the cases they evaluated. A lack of posterior acoustic enhancement and a lack of size allowed USG to miss two cases of simple ganglion, which was different from the current study where US didn't miss any case of ganglion cysts. MRI scans identified simple ganglion cysts in 8 of 8 patients (100%) and solid mass lesions in 3 of 3 patients (100%) in all cases.

In the current study, all patients underwent MRI and US examination while about 9 patients out of 50 underwent arthrography and 13 patients out of 50 underwent US guided techniques with two patients had another session of follow up US guided interventions.

In 1981, **Gompels and Darlington**[15] were the first to report on aspirational direction in the US [15]. A typical US-guided surgery begins with a confirmation and localization of the joint or soft tissue disease. The anatomical and pathological diagnosis given on clinical grounds is often revised after US, which impacts the decision to inject and the location of the injection [16].

Fractures were found in 18 (36% of all joints) by both US and MRI, indicating a high degree of agreement between the two modalities in this investigation. **Hauger *et al.*** [17] validated these findings, noting that although plain films are still the gold standard for diagnosing bone fractures, US has proven able to detect undisplaced fractures or bony avulsions that remain occult radiographically. An ultrasound examination in which the bone surfaces are carefully inspected may provide diagnostic clues.

In contrast to our findings, **Singh *et al.*** [18] observed that high-resolution ultrasound (HRUS) is significantly limited in cases of bony pathologies with its inability of to detect bone edema, avascular necrosis (AVN), and nonunion fracture at the wrist joint. US is an assessor-based approach dependent on assessor learning and competence, which may explain why our results differ.

Three (6%) joints had a radius fracture that was identified by both US and MRI, indicating good agreement between the two modalities in this investigation. In agreement with our findings, **Sultan *et al.*** [19] 78 patients' ultrasound data were analyzed for distal radial fractures and compared to conventional radiographs as the gold standard. The researchers discovered that the ultrasound had a sensitivity of 95.5%, a specificity of 100%, an accuracy of 96.15%, a positive predictive value of 100%, and a negative predictive value of 80% in detecting fractures. However, **Taljanovic *et al.*** [20] 115 demonstrated the necessity for additional imaging studies to always confirm a US diagnosis.

In the present analysis, scapholunate dissociation was observed in two cases (4%), whereas scapholunate

advanced collapse (SLAC) was identified in one case (2 %). The MRI and X-ray and CT scans corroborate the diagnosis received from the MRI.

In the present study, there was a significant agreement between US and MRI regarding the detection of avascular necrosis as it was detected in 11 (22%) joints by both modalities. In 9 (18%) joints, lunate AVN was diagnosed by both US and MRI, showing a high degree of agreement between the two modalities. In their study **Elkhader** [21] showed that US has become a common approach for assessing the musculoskeletal system. It has become a primary diagnostic tool. US revealed avascular necrosis in 8% (14 of 175) of their cases.

Here, researchers found that US and MRI were very much on the same page when it came to identifying extensor tendon involvement. The results of our research corroborate those of **Robinson** [22] to evaluate common tendon anomalies, USG is a fast and reliable imaging technique. To top it all off, its precision in detecting tendon anomalies is on par with that of MRI. Our results are confirmed by **El-Deek *et al.*** [11] who reported that both MRI and USG detected a total of 19 (38%) tendinopathy with high agreement between the two modalities.

Our results disagreed with **El-Sayed *et al.*** [23] who said that MRI could only spot ECU damage in 13 joints whereas US could spot it in 17? Together, they had 13 points of agreement. US discovered four injured joints with ECUs that MRI had missed. There was a 100% sensitivity, an 89.19% specificity, and a 92% accuracy in their study.

With respect to the detection of flexor tendon involvement, the present investigation found that US and MRI were highly congruent. Similar findings were found by US as in **Hmamouchi *et al.*** [24] study, which reported US findings of flexor tenosynovitis in 17 individuals (51.5%) compared to 16 patients (48.5%) on clinical examination.

In the present study, there was a significant agreement between US and MRI regarding the detection of median nerve involvement symptoms of carpal tunnel syndrome (CTS) as it was detected in 7 (14%) joints by both modalities. In agreement with our findings, **Singh *et al.*** [18] documented that accuracy of HRUS is 100% in detecting carpal tunnel thickening.

Ligament tears were found in 5 joints using MRA and 3 using MRI in the current study. Both of them had 3 joints in common agreement. However, MRA was able to identify two joints where MRI had missed ligament tears. In the same context, **Mehta *et al.*** [25] when comparing MRA to the gold standard of wrist arthroscopy for evaluating persistent wrist pain, arthroscopy was found to be more accurate. The diagnostic accuracy of MRA was demonstrated to be higher than that of MRI, leading the authors to the conclusion that MRA is a useful method for assessing persistent wrist pain.

In the present study, about 4 cases out of 50 were known or discovered for first time to have advanced rheumatoid arthritis, both US and MRI agreed in detection of all signs of late rheumatoid arthritis. Our results disagreed with **Issar *et al.*** [26] who evaluated US and MRI 50 rheumatoid arthritis patients were studied to see if there was a connection between their symptoms at the wrist and their metacarpophalangeal joints. Their study showed bone erosions in 14% of US case and 44.8% in MRI, which was statistically significant with P = 0.0001 suggesting that sensitivity of USG is less than MRI. However, they reported that Gray-scale US and Power Doppler US (GSUS, PDUS) evaluation was equal to contrast MRI evaluation in detecting joint space narrowing, effusion, flexor tenosynovitis (except for FPL tendon), extensor tenosynovitis.

In the current study, both MRI and US agreed in detection of bony erosions. Analysis of the data revealed a statistically significant (p 0.0001) correlation between the two methods for identifying erosive arthropathy symptoms. In the same line with our findings, **Singh *et al.*** [18] observed that for bony erosions, US had an accuracy of 87.5% relative to MRI.

In the present study, there was a significant agreement between US and MRI regarding the detection of osteoarthritis changes as it was detected in 14 (28%) joints by both modalities, which matched with **Möller *et al.*** [27] who stated that cartilage damage can be quantified by US in osteoarthritis. In the same line with our results **Singh *et al.*** [18] has shown that HRUS can identify joint effusion, synovitis, synovial hypertrophy, and tenosynovitis much like MRI does.

CONCLUSIONS

US showed promising results regarding the examination of superficial structures of the wrist (both skeletal and soft). Musculoskeletal US is highly advised for assessing wrist tendonitis and inflammatory changes; however, US images of the triangular fibrocartilage and interosseous ligaments do not provide satisfactory information, thus MRI is better for evaluation of internal wrist derangement. US is also highly operator dependent. Also, US is non-invasive, portable, lacks the exposure to ionizing radiation, which is also an advantage of the MRI, and it is of low cost. MRA is highly accurate for the evaluation of TFCC and ligamentous injury of the wrist joint.

Financial support and sponsorship: Nil
Conflict of Interest: Nil.

REFERENCES

1. **Shehab R, Mirabelli M (2013)**: Evaluation and diagnosis of wrist pain: a case-based approach. Am Fam Physician, 87(8):568–573.
2. **Orlandi D, Ferrero G, Fabbro E *et al.* (2013):** Ultrasound (US) guided interventional procedures around the hand and the wrist 2013: European Congress of Radiology-ESSR. Pp.34.doi:

10.1594/essr2013/P-0034

3. **Mandl P, Naredo E, Conaghan P *et al.* (2012):** Practice of ultrasound-guided arthrocentesis and joint injection, including training and implementation, in Europe: results of a survey of experts and scientific societies. Rheumatology (Oxford), 51:184-90.
4. **Koski J, Hammer H (2012):** Ultrasound-guided procedures: techniques and usefulness in controlling inflammation and disease progression. Rheumatology, 51: 31-35.
5. **Berger R, Garcia-Elias M (1991):** General Anatomy of the Wrist. In: An K, Berger R, Cooney W, editors. Biomechanics of the Wrist Joint. New York, NY: Springer New York. Pp. 1-22. https://link.springer.com/chapter/10.1007/978-1-4612-3208-7_1
6. **Standring S (2021):** Gray's anatomy e-book: the anatomical basis of clinical practice. 42nd ed: Elsevier Health Sciences. https://www.elsevier.com/books/gray's-anatomy/978-0-7020-7705-0
7. **Yamamoto A, Huang B, Chung C (2022):** Wrist: Anatomy and MRI Optimization. In: Casagranda BU, editor. MRI of the Upper Extremity: Elbow, Wrist, and Hand. Cham: Springer International Publishing; Pp. 113-32. https://www.scribd.com/book/576596591/MRI-of-the-Upper-Extremity-Elbow-Wrist-and-Hand
8. **El-Kholy M, Maaly M, Hemeeda Y (2015):** Role of MRI in evaluation of painful wrist joint.Menoufia Med J., 28:503-7.
9. **Omar N, Mahmoud M, Saleh W *et al.* (2019):** MR arthrography versus conventional MRI and diagnostic arthroscope in patients with chronic wrist pain. Eur J Radiol Open, 6:265-74.
10. **Kamal H, Abdelsattar M, El-Liethy N (2014):** Evaluation of lesions of the internal ligaments of the wrist; Conventional magnetic resonance imaging versus MR arthrography (MRA). Egypt J Radiol Nucl Med., 45:771-8.
11. **El-Deek A, Dawood E, Mohammed A (2019):** Role of ultrasound versus magnetic resonance imaging in evaluation of non-osseous disorders causing wrist pain. EJRNM., 50: 1-7.
12. **Singh K, Thukral C, Gupta K (2017):** Tendo-ligamentous pathologies of the wrist joint: Can ultrasonography replace magnetic resonance imaging? EJRNM., 48:15-8.
13. **Kadry O, Algebally A, Almassry H *et al.* (2021):** Assessment of triangular fibro- cartilaginous complex injuries of the wrist using high resolution ultrasound versus magnetic resonance imaging. Egypt J Hosp Med., 85:4092-5.
14. **Kadah R, Elsaid N, Fatah M (2016):** Triangular fibrocartilage and ligamentous injury of the wrist joint: Does MR arthrography improve diagnosis over standard MRI? EJRNM., 47:1501– 9.
15. **Gompels B, Darlington L (1981):** Septic arthritis in rheumatoid disease causing bilateral shoulder dislocation: diagnosis and treatment assisted by grey scale ultrasonography. Ann Rheum Dis., 40: 609-11.
16. **Kane D, Koski J (2016):** Musculoskeletal interventional procedures: With or without imaging guidance? Best Practice & Research Clinical Rheumatology, 30:736-50.
17. **Hauger O, Chung C, Lektrakul N *et al.* (2000):** Pulley system in the fingers: normal anatomy and simulated lesions in cadavers at MR imaging, CT, and US with and without contrast material distention of the tendon sheath. Radiology, 217: 201-212.
18. **Singh A, Rastogi R, Khare V *et al.* (2021):** Comparative evaluation of high- resolution ultrasonography and magnetic resonance imaging in painful wrist joint. Acta Medica International, 8:38-43.
19. **Sultan A, Abdul Aziz M, Alsaleem Y (2017):** Accuracy of diagnosis of distal radial fractures by ultrasound. Egypt J Hosp Med., 69:3115-22.
20. **Taljanovic M, Sheppard J, Jones M *et al.* (2008):** Sonography and sonoarthrography of the scapholunate and lunotriquetral ligaments and TFC: Initial experience and correlation with arthrography and magnetic resonance arthrography. J Ultrasound Med., 27(2): 179-91.
21. **Elkhader B (2022):** Sonography of the wrist joint: Pathologic conditions. MSARR., 04:5– 10.
22. **Robinson P (2009):** Sonography of common tendon injuries. AJR Am J Roentgenol., 193:607-18.
23. **El-Sayed M, El-Azizi A, Shahin A *et al.* (2020):** High resolution ultrasound vs MRI in evaluation of triangular fibrocartilage complex. Med J Cairo Univ., 85:2109-13.
24. **Hmamouchi I, Bahiri R, Srifi N *et al.* (2011):** A comparison of ultrasound and clinical examination in the detection of flexor tenosynovitis in early arthritis. BMC Musculoskelet Disord., 12: 91-92.
25. **Mehta N, Garg B, Ansari T *et al.* (2019):** Comparison of magnetic resonance arthrography and wrist arthroscopy in the evaluation of chronic wrist pain in Indian population. Indian J Orthop., 53:769-75.
26. **Issar P, Nadiger V, Hiran S *et al.* (2016):** Ultrasound and magnetic resonance imaging correlation of the wrist and metacarpophalangeal joints in fifty consecutive patients of rheumatoid arthritis. Indian J Rheumatol., 11:186-91.
27. **Möller B, Bonel H, Rotzetter M *et al.* (2009):** Measuring finger joint cartilage by ultrasound as a promising alternative to conventional radiograph imaging. Arthritis Rheum., 61:435-41.